

Modulation of Transducin GTPase Activity by Chimeric RGS16 and RGS9 Regulators of G Protein Signaling and the Effector Molecule[†]

Randall L. McEntaffer, Michael Natochin, and Nikolai O. Artemyev*

Department of Physiology and Biophysics, University of Iowa College of Medicine, Iowa City, Iowa 52242

Received November 5, 1998; Revised Manuscript Received January 21, 1999

ABSTRACT: RGS9, a member of the family of regulators of G protein signaling (RGS), serves as a GTPase-activating protein (GAP) for the transducin α -subunit (Gt α) in the vertebrate visual transduction cascade. The GAP activity of RGS9 is uniquely potentiated by the γ -subunit of the effector enzyme, cGMP-phosphodiesterase (P γ). In contrast, P γ attenuates the GAP effects of several other RGS proteins, including RGS16. We demonstrate here that the P γ subunit exerts its effects on the GTPase activity of the Gt α –RGS complex via the C-terminal domain, P γ -63–87. The structural determinants that control the direction of P γ effects on the RGS–Gt α system are localized within the RGS domains. The addition of P γ caused an increase in the maximal stimulation of Gt α GTPase activity by RGS9d without affecting the EC₅₀ value. Modulation of Gt α GTPase activity by chimeric RGS16 and RGS9 proteins and P γ has been investigated. This analysis suggests that in addition to the differences in primary structures, the overall conformations of the RGS fold in RGS9 and RGS16 are likely to be responsible for the opposite effects of P γ on the RGS9 and RGS16 GAP activity. The RGS9 α 3– α 5 region constituted the minimal insertion of the RGS9 domain into RGS16 that reversed the inhibitory effect of P γ . A model of the RGS9 complex with Gt α shows the α 3– α 5 helices in RGS9 facing the proximate P γ binding site on Gt α . Our results and this model demonstrate that the mechanism of potentiation of RGS9 GAP activity by P γ involves a more rigid stabilization of the Gt α switch regions when Gt α is bound to both RGS9 and P γ .

Recently, a novel class of GTPase-activating proteins for heterotrimeric G proteins termed regulators of G protein signaling (RGS)¹ has been described (1–3). Members of the RGS family negatively regulate G protein signaling of G proteins, particularly those from Gi, Gq, and G12 families (4–7). RGS proteins share a conserved RGS domain, which is responsible for their GAP activity (4–6). RGS domains bind to the conformation-sensitive switch regions of the G α subunits when the latter assume a transitional state for GTP hydrolysis (8, 9). The G α 's GTPase activity is accelerated as a result of stabilization of the transitional state. This mechanism of the RGS GAP function is supported by the first crystal structure of RGS4 bound to Gt α 1AlF₄[–] (10).

The discovery of RGS proteins has had important implications for the visual transduction cascade. During photoexcitation, the transducin α -subunit (Gt α) in the active GTP-bound conformation stimulates the effector enzyme, cGMP phosphodiesterase (PDE), by displacing the inhibitory γ -subunits (P γ) from the PDE catalytic core (P α β) (11–13).

Intrinsic Gt α GTPase activity leads to inactivation of transducin, which is central to the turnoff of the cascade (14). Until recently, one of the major unresolved questions has been a discrepancy between the slow rate of the Gt α GTPase activity measured in vitro and the fast photoresponse turnoff in mammalian rods in vivo (15–18). It was long thought that the existence of a GAP for Gt α might explain this inconsistency. The effector molecule, and more specifically the P γ subunit, had become an early candidate for such a GAP (19). However, subsequent studies have established that a distinct membrane-associated factor is the principal GAP in phototransduction, whereas P γ enhances this factor's GAP activity toward Gt α (20, 21). Hypothesizing that the GAP factor might belong to the RGS family, several groups have cloned a number of retina-specific RGS proteins such as mRGSr (RGS16), RET-RGS1, and RGS9, which are capable of stimulating Gt α GTPase activity (22–24). Although a retinal localization of RGS16 has been shown by Northern analysis (22), the presence of the RGS16 protein in photoreceptor cells has not been demonstrated. In our experiments, a specific antibody capable of detecting 0.1 ng of RGS16 failed to identify this RGS in the fraction of rod outer segment membranes (unpublished results). Evidence suggests that RGS9 is the one at work in the visual transduction cascade (24). In retina, RGS9 is localized in the rod and cone outer segments of photoreceptor cells, in which it colocalizes with other phototransduction components (24, 25). Furthermore, the GAP activity of RGS9 for transducin is potentiated by P γ , thus matching the properties of the membrane GAP factor (20, 24, 25). Potentiation of the RGS9

[†] This work was supported by National Institutes of Health Grant 2RO1 EY-10843 and American Heart Association Grant-in-Aid 9750334N. NIH Grant DK-25295 supported the services provided by the Diabetes and Endocrinology Research Center of the University of Iowa. M.N. is a recipient of the American Heart Association Iowa Affiliate Postdoctoral Fellowship.

* To whom correspondence should be addressed. Telephone: (319) 335-7864. Fax: (319) 335-7330. E-mail: Nikolai-Artemyev@UIOWA.EDU.

¹ Abbreviations: RGS proteins, regulators of G protein signaling; RGS16d and RGS9d, RGS domains of RGS16 and RGS9, respectively; GAP, GTPase-activating protein; ROS, rod outer segment(s); uROS, urea-washed ROS membranes.

action by $P\gamma$ implies simultaneous binding of the two molecules to $G\alpha$. The potentiation of RGS9 GAP activity by $P\gamma$ may constitute an important feedback mechanism by which the activated effector contributes to signal termination.

The synergistic effect of RGS9 and $P\gamma$ in stimulating the $G\alpha$ GTPase activity is unique, because acceleration of $G\alpha$ GTPase by other tested RGS proteins such as RGS16, RGS4, and GAIP is attenuated by $P\gamma$ (26–28). This attenuation appears to be allosteric and results from the noncompetitive binding of $P\gamma$ and RGS to $G\alpha$ (27). Despite an apparent lack of physiological relevance, the inhibition of RGS16 GAP activity by $P\gamma$ represents an interesting model interaction that can be utilized to probe the mechanism of regulation of the RGS9 function by $P\gamma$. Here, we analyze the structural determinants of RGS9 that contribute to the synergism between RGS9 and $P\gamma$ using chimeric RGS16 and RGS9 proteins.

EXPERIMENTAL PROCEDURES

Preparation of Rod Outer Segment (ROS) Membranes, $G\alpha\beta\gamma$, $P\gamma$, and RGS16. Bovine ROS membranes were prepared as previously described (29). Urea-washed ROS membranes (uROS) were prepared according to a previously published protocol (30). $G\alpha\beta\gamma$ was prepared by a previously described procedure (31). Recombinant $P\gamma$ was expressed in *Escherichia coli* and purified according to a previously published protocol (32). Peptides corresponding to residues 24–45 and 63–87 of $P\gamma$ were synthesized and purified as previously described (32). RGS16 was prepared and purified as described in ref 27.

Cloning and Site-Directed Mutagenesis of RGS16d, RGS9d, and Chimeric RGS16–RGS9 Proteins. cDNA encoding the RGS domain of RGS16 (RGS16d, amino acids 61–180) was PCR amplified from the pGEX-KG-RGS16 vector (27) using primers carrying the *Xba*I and *Xho*I restriction sites and subcloned into the pGEX-KG vector (33). RGS16d was expressed and purified according to a previously published protocol (27). cDNA encoding the RGS domain of RGS9 [amino acids 291–418 of RGS9 (24)] was PCR amplified from the human retinal cDNA library (provided by J. Nathans, Johns Hopkins University, Baltimore, MD) using primers carrying the *Nde*I and *Bam*HI restriction sites. The PCR product was subcloned into the pET15b vector for expression of RGS9d as a His-tagged protein in *E. coli*. RGS9d was expressed and purified essentially as described by He et al. (24).

Two silent restriction sites (*Avr*II and *Afl*III) were introduced at the start (Gly61) and near the end (Leu172) of the RGS16d cDNA. The RGS sequences outside RGS16d were PCR amplified and then used as primers in the second round of PCR amplification with RGS16 cDNA as a template. To obtain the first chimera (C1), RGS9d was amplified with primers containing *Avr*II and *Afl*III sites and subcloned into the pGEX-KG-RGS16 vector cut with *Avr*II and *Afl*III to replace RGS16d (C1, 1–61RGS16/296–408RGS9/176–202RGS16). Next, a silent *Nde*I restriction site was introduced into RGS16 cDNA (Ile122) using two-round PCR amplifications as described above. A cDNA segment encoding the C-terminal half of the RGS9d residues (357–408 of RGS9) was PCR amplified using a 5' primer containing an *Nde*I site and a 3' primer with an *Afl*III site. This PCR

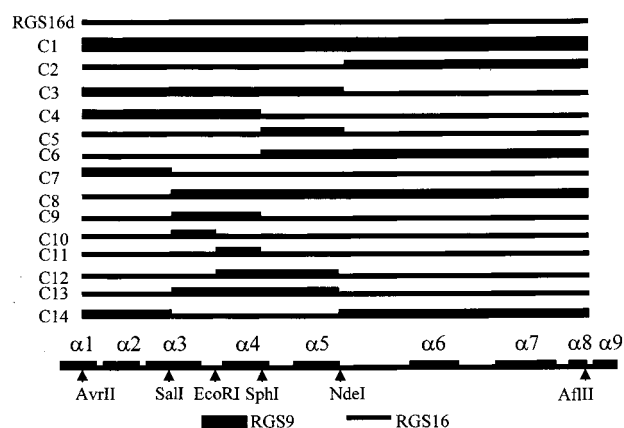


FIGURE 1: Schematic representation of RGS domains of chimeric RGS16–RGS9 proteins. Restriction sites that were utilized in cloning of the RGS16–RGS9 chimeras are denoted.

fragment and pGEX-KG-RGS16 were digested using *Nde*I and *Afl*III and then ligated together to produce chimera C2 (1–123RGS16/357–408RGS9/176–202RGS16). Chimera C3 containing the N-terminal half of RGS9d was generated in a manner similar to that of C2 using the *Avr*II and *Nde*I sites (C3, 1–61RGS16/296–354RGS9/122–202RGS16). A silent *Sph*I site was introduced in both RGS9 and RGS16 cDNAs to generate chimeric RGS proteins C4–C6 (Figure 1). This restriction site provided junctions Cys98RGS16/Glu333RGS9 and Cys332RGS9/Glu99RGS16 in these chimeras. A *Sal*I site, introduced into the RGS16 cDNA and intrinsic to the RGS9d cDNA, along with the previous restriction sites was used to construct chimeric RGS proteins C7–C9. The *Sal*I site allowed the joining of RGS16 and RGS9 sequences at Gly75RGS16/Arg310RGS9 or Gln311RGS9/Ala78RGS16. To further the development of chimeric proteins, an *Eco*RI site, which is already present in the RGS9d cDNA, was silently introduced into the RGS16 cDNA. The *Eco*RI site furnished junctions Glu320RGS9/Phe87RGS16 in chimeric protein C10 and Glu86RGS16/Phe321RGS9 in C11 and C12. The *Sal*I and *Nde*I restriction sites were used to generate chimeras 13 and 14. Single point mutations of RGS16, Glu89Gly, Glu93Gly, and Leu96Glu, were introduced by PCR-directed mutagenesis using primers carrying the mutation and an *Sph*I restriction site. All generated sequences were verified by automated DNA sequencing at the University of Iowa DNA Core Facility.

Single-Turnover GTPase Assays. Single-turnover GTPase assays were carried out in suspensions of uROS (5 μ M R*) reconstituted with 0.4 μ M Gt in 20 mM HEPES buffer (pH 7.4) containing 100 mM NaCl and 8 mM $MgSO_4$ essentially as described previously (24). The GTPase reactions were initiated by addition of 100 nM [γ - ^{32}P]GTP ($\sim 5 \times 10^4$ dpm/pmol). After a 5 s interval, one of the RGS proteins (RGS9, RGS16, or chimeric RGS9–RGS16) and $P\gamma$ or $P\gamma$ peptides were added. The reactions proceeded for another 5 s and were quenched by addition of 100 μ L of 7% perchloric acid. Nucleotides were then precipitated using charcoal, and the amount of free $^{32}P_i$ that formed was measured by liquid scintillation counting. The results are expressed as the mean \pm standard error of triplicate measurements. The GTP hydrolysis rate constants were calculated using the method of He et al. (24).

Other Methods. Protein concentrations were determined by the method of Bradford (34) using IgG as a standard or

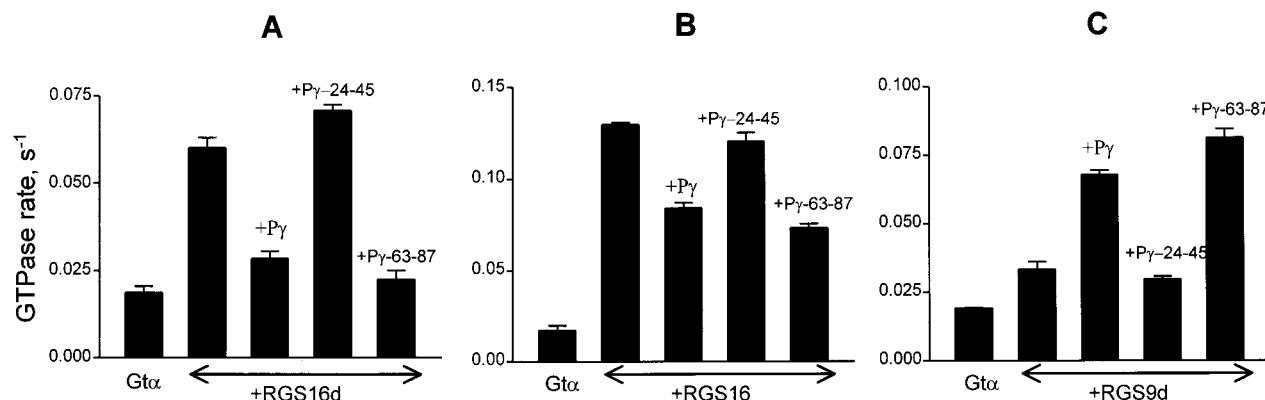


FIGURE 2: Modulation of Gtα GTPase activity by RGS16d, RGS16, and RGS9d in the absence or in the presence of Pγ, Pγ-24-45 or Pγ-63-87. Single-turnover GTPase assays were carried out in suspensions of uROS (5 μM R*) reconstituted with 0.4 μM Gt as described in Experimental Procedures. RGS16d (0.5 μM), RGS16 (0.5 μM), or RGS9d (3 μM) was added with or without Pγ (1 μM), Pγ-24-45 or Pγ-63-87 (50 μM each).

using calculated extinction coefficients at 280 nm. Rhodopsin concentrations were measured using the difference in absorbance at 500 nm between “dark” and bleached ROS preparations. The modeling of the Gtα–RGS9 complex was performed using SWISS-MODEL (35) and coordinates of the RGS4–Gtα₁ complex as a template (10).

RESULTS

Effect of Pγ on Stimulation of Gtα GTPase Activity by the RGS Domains of RGS16 and RGS9. We and others have previously demonstrated the inhibitory effects of Pγ on the GAP activity of RGS16 toward Gtα (26, 27). To determine whether the RGS domain of RGS16 is responsible for this modulation by Pγ, we have tested how Pγ affects stimulation of Gtα GTPase activity by RGS16d. Single-turnover assays were carried out as described in Experimental Procedures. Figure 2A shows that RGS16d at a concentration of 0.5 μM stimulated Gtα GTPase activity by ~3.5-fold. Addition of 1 μM Pγ inhibited this stimulation in a manner similar to that of the effect of Pγ on the GAP activity of full-length RGS16 (Figure 2B). This rules out the possibility that the inhibitory effect of Pγ on RGS16 GAP activity might be mediated by the sequences outside the RGS domain. We then confirmed the potentiation of the RGS9d GAP effect on Gtα by Pγ. In our experiments, RGS9d maximally accelerated the GTPase activity of Gt reconstituted with uROS membranes by ~3.5-fold with an EC₅₀ value of 3 μM (Figure 3). Effects of Pγ on Gtα GTPase activity were subsequently tested under conditions of half-maximal stimulation by RGS9d. The addition of increasing concentrations of Pγ brought the RGS9d-stimulated Gtα GTPase activity up further in a dose-dependent manner (not shown). The Gtα GTPase rate in the presence of 3 μM RGS9d reached a maximal level (~0.07 s⁻¹) at 1 μM Pγ (Figure 2C). Thereafter, this concentration of Pγ was fixed when examining the modulation of RGS9d and chimeric RGS16–RGS9 by Pγ. The above results are consistent with previous observations (24, 27) and demonstrate that the structural determinants within the RGS domains of different RGS proteins underlie both the attenuation and enhancement of the RGS GAP activity by Pγ.

Effects of Pγ Peptides on the RGS9d and RGS16d GAP Activity. Two major regions of Pγ, a polycationic region (Pγ-24–45) and the C-terminal region (Pγ-63–76), have been

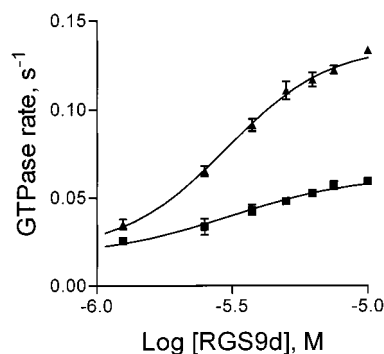


FIGURE 3: Effects of Pγ on dose-dependent stimulation of Gtα GTPase activity by RGS9d. The Gtα GTPase rate constants were determined for GTP hydrolysis in suspensions of uROS (5 μM R*) reconstituted with 0.4 μM Gt and increasing concentrations of RGS9d in the absence (■) or in the presence (▲) of 1 μM Pγ. The calculated EC₅₀ and V_{max} values are (■) 3.1 ± 0.1 μM and 0.065 ± 0.005 s⁻¹ and (▲) 3.0 ± 0.1 μM and 0.14 ± 0.01 s⁻¹, respectively.

implicated in the interaction with Gtα (32, 36–38). We examined the effects of two synthetic peptides, corresponding to Pγ-24–45 and Pγ-63–87, on the stimulation of Gtα GTPase activity by RGS16, RGS16d, and RGS9d. Peptide Pγ-24–45 had no effect on the degree to which RGS16d, RGS16, or RGS9d accelerated Gtα GTPase activity (Figure 2). The C-terminal peptide, Pγ-63–87, reversed the stimulation of Gtα GTPase activity by RGS16d or RGS16, and enhanced the GAP effect of RGS9d in a manner similar to that of the effects of the full-length Pγ (Figure 2). These results suggest that the C-terminal domain of Pγ is responsible for opposite modulation of the RGS9 and RGS16 GAP activity.

Pγ Enhances the Maximal Stimulation of Gtα GTPase Activity by RGS9d. Potentiation of the GAP activity of RGS9d by Pγ may involve changes in the maximal GTPase activity, the EC₅₀ value, or both of the parameters. To elucidate the mechanism of Pγ action, the extent of stimulation of Gtα GTPase activity by varying concentrations of RGS9d was measured in the absence or in the presence of Pγ (1 μM). The dose dependence curves shown in Figure 3 indicate that the addition of Pγ leads to an increase of the maximal RGS9d-stimulated Gtα GTPase rate (V_{max} effect), whereas the EC₅₀ value (3 μM) remains unchanged.

The single-turnover GTPase assay used in this study does not allow accurate measurements of GTPase rates exceeding

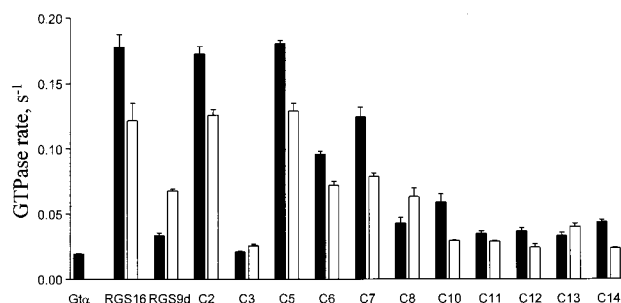


FIGURE 4: Modulation of Gt α GTPase activity by chimeric RGS16–RGS9 proteins and Py. Single-turnover GTPase assays were carried out in suspensions of uROS (5 μ M R*) reconstituted with 0.4 μ M Gt and 3 μ M RGS protein in the absence (black bars) or in the presence (white bars) of 1 μ M Py.

0.2 s⁻¹. At such rates, nearly all the GTP is hydrolyzed after the 10 s incubation period. RGS16 (or RGS16d) is a significantly more potent GAP than RGS9d and at high concentrations can stimulate Gt α GTPase activity to rates of >0.2 s⁻¹. Therefore, we were unable to obtain saturating dose dependence curves for the GTPase rates using RGS16, and consequently determine the effect of Py on the EC₅₀ value for the GAP activity of RGS16. However, a reversal of stimulation of the Gt α GTPase activity by RGS16 at saturating Py concentrations was only partial (50–60%), suggesting an allosteric nature of the Py effect (not shown). Similar observations have been made for Gt α regulation by RGS4 (28).

Modulation of Gt α GTPase Activity by Chimeric RGS9–RGS16 Proteins. Since the RGS domains of RGS9 and RGS16 are fully sufficient for reconstitution of modulation of these RGS proteins by Py, the simplest design would be to generate chimeric RGS16d–RGS9d domains. We have noticed, however, that RGS9d is unstable and has a tendency to slowly precipitate out of solution. Perhaps it is related to the fact that it cannot be expressed as a soluble protein and requires refolding after solubilization of inclusion bodies in 6 M guanidinium chloride (24). This instability of RGS9d prevented us from taking a straightforward approach to making chimeric RGS domains by swapping pieces of RGS16d and RGS9d. Instead, we used full-length RGS16 as a background for substitution of different RGS16d segments with corresponding sequences from RGS9. The first chimeric RGS protein (C1) that was made contained RGS9d flanked by the N- and C-terminal regions of RGS16 (Figure 1). Expression of C1 led to an insoluble protein found exclusively in inclusion bodies. Attempts to increase the solubility of the protein by decreasing the induction temperature to 25 °C and adding 2.5 mM betaine and 1 M sorbitol (39) were unsuccessful. Next, two chimeric RGS proteins, C2 and C3, were generated (Figure 1). C2 was fully functional with a GAP activity comparable to that for RGS16 (Figure 4). Py inhibited the GAP effect of C2 on Gt α . C3 had no GAP activity. However, a small increase (~30%) in the Gt α GTPase activity was detected in the presence of both C3 and Py (Figure 4). Chimeras C2 and C3 thus provided an indication that the N-terminal portion of RGS9d (helices 1–5) may contribute to the RGS9 ability to stimulate the Gt α GTPase activity in concert with Py. To further delineate this region, chimeric RGS proteins C4–C6 were subsequently cloned (Figure 1). C4 was inactive, but C5 and C6 were functionally active (Figure 4). Py negatively modulated

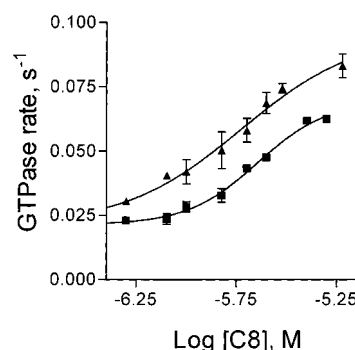


FIGURE 5: Effects of Py on dose-dependent stimulation of Gt α GTPase activity by chimeric RGS, C8. The Gt α GTPase rate constants were determined for GTP hydrolysis in suspensions of uROS (5 μ M R*) reconstituted with 0.4 μ M Gt and increasing concentrations of chimera C8 in the absence (■) or in the presence (▲) of 1 μ M Py. The calculated EC₅₀ and V_{max} values are (■) 2.3 \pm 0.1 μ M and 0.070 \pm 0.005 s⁻¹ and (▲) 1.9 \pm 0.1 μ M and 0.10 \pm 0.01 s⁻¹, respectively.

the C5 and C6 GAP activity toward Gt α , thus excluding the α 5 helix alone as well as the whole α 5– α 8 region of RGS9 as domains that are responsible for the synergistic GAP effect of RGS9 and Py. Chimera C7 was made to probe the role of the RGS9 α 1– α 2 region (Figure 1). C7 appeared to be functionally equivalent to the wild-type RGS16, indicating that the α 1– α 2 region is not involved in the modulation of the RGS GAP activity by Py (Figure 4). This result was also corroborated by C8 (Figure 1). The GAP effect of C8 was enhanced in the presence of Py by ~50% (Figure 4). These results seemed to implicate the RGS α 3 and α 4 helices. Therefore, a chimeric RGS protein, C9, containing the RGS9 α 3– α 4 region was designed to elucidate the role of this region (Figure 1). However, C9 was inactive. The α 3– α 4 region was further split in chimeric proteins C10 and C11, which contained individual helices α 3 and α 4 of RGS9, respectively. Although C11 was relatively inefficient in stimulating Gt α GTPase activity, both C10 and C11 were negatively modulated by Py (Figure 4). In addition, we have made a chimeric RGS protein containing the α 4– α 5 region of RGS9d (C12). C12 displayed functional characteristics similar to those of C11, i.e., modest stimulation of Gt α GTPase activity, which was attenuated by Py. Hence, the overall data indicate that whereas the N-terminal half of RGS9d (α 1– α 5) is apparently involved in the synergistic potentiation of the RGS9 GAP activity by Py, none of the individual domains (α 1– α 2, α 3, α 4, α 5, and α 4– α 5) was sufficient to reproduce this effect in the context of RGS16. However, a modest but consistent enhancement of Gt α GTPase activity by Py was observed for chimera C13 (Figure 1), which contains three α -helices, α 3– α 5, and the connecting loops from RGS9 (amino acids 310–354) (Figure 4). Supporting the requirement for the α 3– α 5 helices in the Py modulation of RGS, a symmetrical chimera C14 which contained the α 3– α 5 helices from RGS16d exhibited negative regulation by Py (Figure 4).

To examine how closely the chimeric RGS16–RGS9 proteins that displayed RGS9d-like modulation reflect the functional properties of RGS9d, the representative chimera, C8, has been analyzed in the titration experiments. Figure 5 shows that C8 activated Gt α GTPase activity in a manner analogous to that of RGS9d with a maximal stimulation of ~3.5-fold and an EC₅₀ value of 2.3 μ M. The extent of

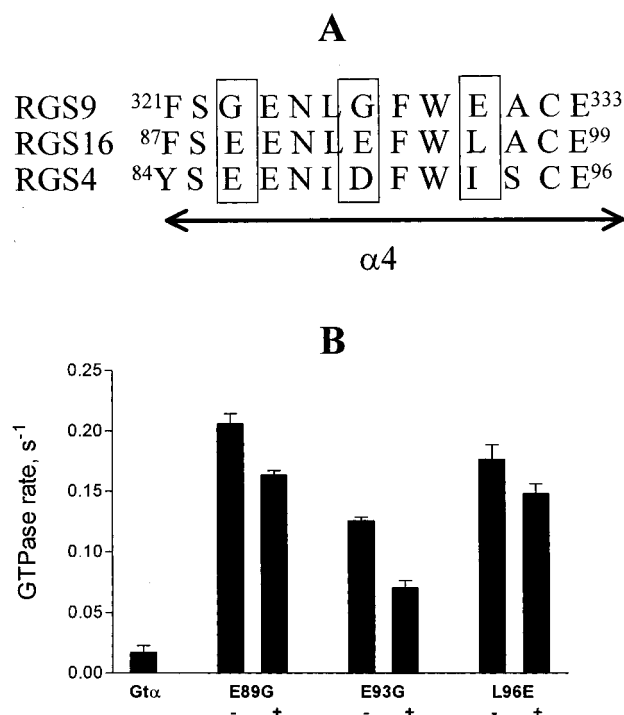


FIGURE 6: (A) Sequence alignment of the $\alpha 4$ helices from RGS domains of RGS9, RGS16, and RGS4. Nonconserved residues are denoted. (B) Effects of point mutants of RGS16 and $P\gamma$ on $G\alpha$ GTPase activity. Point mutants of RGS16 with substitutions of nonconserved $\alpha 4$ residues with the corresponding RGS9 residues were tested in single-turnover GTPase assays in suspensions of uROS ($5 \mu\text{M}$ R*) reconstituted with $0.4 \mu\text{M}$ Gt and $0.5 \mu\text{M}$ mutant RGS16 in the absence (–) or in the presence (+) of $1 \mu\text{M}$ $P\gamma$.

potentiation of C8 GAP activity by $P\gamma$ was somewhat lower than that of RGS9d (Figure 5). Nonetheless, the EC_{50} value for the GTPase activation by C8 in the presence of $P\gamma$ was practically unaffected ($EC_{50} = 1.9 \mu\text{M}$) as it was seen for the RGS9d effect.

Some of the examined chimeric RGS16–RGS9 proteins were inactive (C1, C4, and C9), indicating incorrect folding of the RGS domain. Several other chimeras, such as C3 and C11–C13, had weak GAP activity toward $G\alpha$. This in part may be due to the relatively inefficient GAP activity of RGS9d, although the altered folding of the chimeric RGS domain may contribute as well. Analysis of the GAP activity of chimeric RGS suggests that those chimeras that contained the RGS9d $\alpha 4$ helix were most impaired. Therefore, the chimeric approach could have left unnoticed the potential structural elements within the $\alpha 4$ helix that are required for the synergistic effects of RGS9 and $P\gamma$. An alignment of the $\alpha 4$ sequences from RGS16, RGS4 (both are inhibited by $P\gamma$), and RGS9 (potentiated by $P\gamma$) reveals three non-conservative positions (Figure 6A). Reflecting these differences, three RGS16 mutants, Glu89Gly, Glu93Gly, and Leu96Glu, with single substitutions for RGS9 residues have been made. All three mutants stimulated $G\alpha$ GTPase activity in a manner similar to that of RGS16 (Figure 6B). Furthermore, $P\gamma$ attenuated the GAP activity of these mutants in a manner analogous to that of RGS16 (Figure 6B).

DISCUSSION

Rapidly accumulating evidence indicates an important role of RGS proteins in regulation of a variety of cellular mechanisms mediated by G proteins (4–6). RGS proteins are very diverse and may contain multiple structural domains. The presence of the RGS domain is a common denominator that allows grouping of all these proteins into one large family. The crystal structure of RGS4 bound to $G\alpha_1\text{AlF}_4^-$ has elucidated a general architecture of the RGS domain and a principle mechanism of the RGS GAP activity (10). The conserved RGS core is composed of nine α -helices that fold into two subdomains. The larger subdomain which includes helices $\alpha 3$ – $\alpha 8$ is a typical antiparallel four-helix bundle. Loops $\alpha 3$ – $\alpha 4$ and $\alpha 5$ – $\alpha 6$ and the region of $\alpha 7$ – $\alpha 8$ form

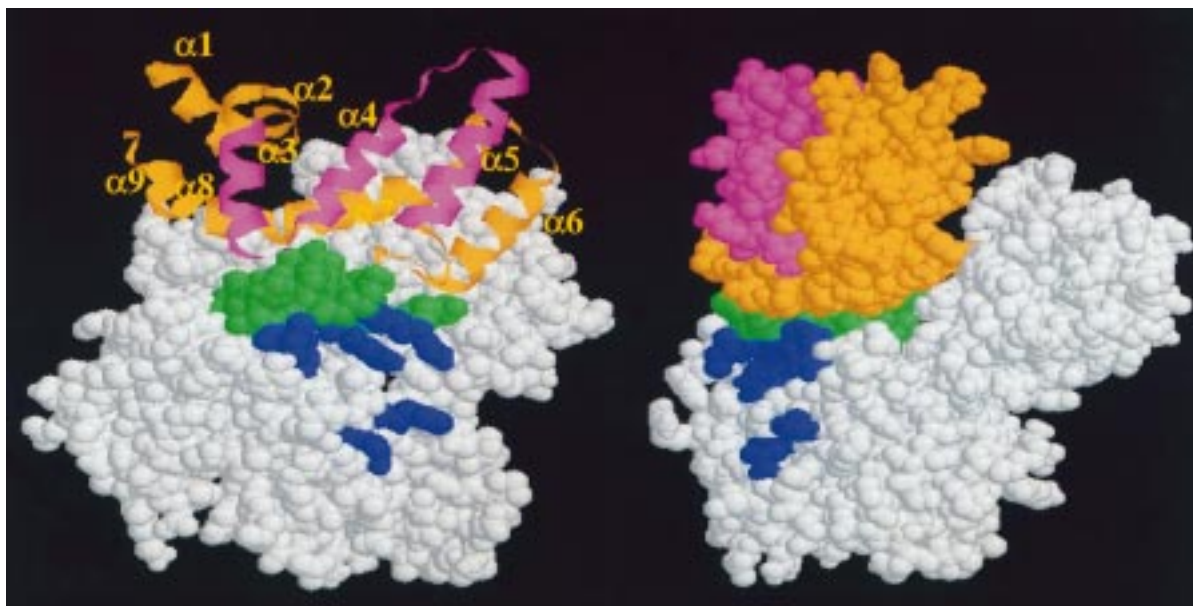


FIGURE 7: Model of the complex between RGS9d and $G\alpha$. (Left) The RGS9d– $G\alpha$ complex was modeled using SWISS-MODEL (35) and the RGS4– $G\alpha_1$ crystal structure (10) as a template. The picture was generated using RasMol (version 2.6). The RGS9 contact residues of $G\alpha$ are green. Effector-interacting residues from the switch II region and the $\alpha 3$ helix of $G\alpha$ (40) are blue. The $\alpha 3$ – $\alpha 5$ region of RGS9d (amino acids 310–354) is magenta; the remaining RGS9d residues are orange. (Right) View of the complex rotated 90° around the vertical axis with respect to the view in the left panel. The RGS9d chain is shown in a space-filling mode.

three distinct sites of interaction with G α . These RGS regions make contacts with the three switch regions of G α_1 (10). Interaction of RGS protein with the G protein switch regions suggests a reduction in the free energy of the transitional state via stabilization of G α switch regions and residues directly involved in GTP hydrolysis as the mechanism of RGS GAP activity (10). Recently, we identified G α residues that are critical for the interaction with the P γ subunit of the effector enzyme, PDE (40). Comparative analysis of the RGS and effector interfaces of G α allows for speculation about the mechanism of potentiation of RGS9 GAP action by P γ . We have shown that RGS and P γ bind to distinct G α residues located in close proximity within the switch II region (40). Such an organization of the two interfaces may have several functional consequences. Noncompetitive binding of P γ to the RGS9–G α complex may lead to further stabilization of the switch II region, and therefore to the enhanced G α GTPase activity. This would explain why P γ does not act alone as a GAP but rather serves as a cofactor for RGS9. P γ binds almost equally well to the GTP γ S-bound G α and to the transitional state mimicked by the AlF $_4^-$ conformation (41), whereas RGS proteins prefer the latter conformation (8–10). Moreover, the close proximity of P γ and RGS9 in the complex with G α may lead to an interaction between P γ and RGS9. As a result, RGS9 may have a higher affinity for the P γ –G α complex, also explaining the P γ potentiation effect. Our data suggest that P γ increases the maximal RGS9d-stimulated rate of G α GTPase activity without affecting the affinity of RGS9d for G α . This finding favors a more rigid stabilization of the G α switch regions in a trimeric complex, RGS9–G α –P γ , rather than an interaction between RGS9 and P γ as the mechanism underlying the synergistic effects of RGS9 and P γ on G α . At present, there is no evidence suggesting that RGS9 and P γ may interact. Our efforts to detect a potential interaction between P γ and RGS9d using fluorescence binding assays were unsuccessful (unpublished observations). The attenuation of RGS16 or RGS4 can also be rationalized in terms of the close proximity of these RGS proteins and P γ in the trimeric complex with G α . A repulsive interaction or a steric hindrance between RGS16 (RGS4) and P γ may lead to less efficient stabilization of the G α switch regions, and consequently to the lower GAP activity.

The analysis of modulation of the G α GTPase activity by chimeric RGS16–RGS9 proteins and P γ first implicated the N-terminal half (α 1– α 5) of the RGS domain in the opposite regulation of RGS9 and RGS16 by P γ . However, substitutions of the individual RGS16d α -helices and loops within this region by corresponding segments of RGS9d did not reverse the inhibitory effect of P γ on the GAP activity of such chimeric proteins. The minimal insert of RGS9 into RGS16 that resulted in the potentiation of chimeric RGS by P γ was the α 3– α 5 segment. This result suggests that an overall conformation of the RGS9d α 3– α 5 region (tilts and angles of the α 3– α 5 helices and forms of the connecting loops) is important for allowing a synergism between RGS9 and P γ . Alternatively, a combination of multiple residues within the α 3– α 5 region of RGS9d may contribute to the unique properties of RGS9. A model of the RGS9–G α complex, generated using a crystal structure of the complex of RGS4 with G α_1 as a template (10), is shown in Figure 7. Interestingly, the RGS9 α 3– α 5 helices and the connecting

loops are facing the P γ binding surface on G α identified by site-directed mutagenesis of G α (40). Perhaps the opposite effects of P γ on RGS9 and RGS16 can be explained simply by the lack of interference between the RGS9 α 3– α 5 region and P γ , thus allowing for optimal stabilization of the G α switch regions in the RGS9–G α –P γ complex.

REFERENCES

1. Koelle, M. R., and Horvitz, H. R. (1996) *Cell* 84, 115–125.
2. Druey, K. M., Blumer, K. J., Kang, V. H., and Kehrl, J. H. (1996) *Nature* 379, 742–746.
3. Berman, D. M., Wilkie, T. M., and Gilman, A. G. (1996) *Cell* 86, 445–452.
4. Dohlman, H. G., and Thorner, J. (1997) *J. Biol. Chem.* 272, 3871–3874.
5. Koelle, M. R. (1997) *Curr. Opin. Cell Biol.* 9, 143–147.
6. Berman, D. M., and Gilman, A. G. (1998) *J. Biol. Chem.* 273, 1269–1272.
7. Kozasa, T., Jiang, X., Hart, M. J., Sternweis, P. M., Singer, W. D., Gilman, A. G., Bollag, G., and Sternweis, P. C. (1998) *Science* 280, 2109–2111.
8. Berman, D. M., Kozasa, T., and Gilman, A. G. (1996) *J. Biol. Chem.* 271, 27209–27212.
9. Watson, N., Linder, M. E., Druey, K. M., Kehrl, J. H., and Blumer, K. J. (1996) *Nature* 383, 172–175.
10. Tesmer, J. J. G., Berman, D. M., Gilman, A. G., and Sprang, S. R. (1997) *Cell* 89, 251–261.
11. Chabre, M., and Deterre, P. (1989) *Eur. J. Biochem.* 179, 255–266.
12. Yarfitz, S., and Hurley, J. B. (1994) *J. Biol. Chem.* 269, 14329–14332.
13. Stryer, L. (1996) *Proc. Natl. Acad. Sci. U.S.A.* 93, 557–559.
14. Sagoo, M. S., and Lagnado, L. (1997) *Nature* 389, 392–395.
15. Fung, B. K.-K., Hurley, J. B., and Stryer, L. (1981) *Proc. Natl. Acad. Sci. U.S.A.* 78, 152–156.
16. Baehr, W., Morita, E., Swanson, R., and Applebury, M. L. (1982) *J. Biol. Chem.* 257, 6452–6460.
17. Sitaramayya, A., and Liebman, P. A. (1983) *J. Biol. Chem.* 258, 12106–12109.
18. Hodgkin, A. L., and Nunn, B. J. (1988) *J. Physiol.* 403, 439–471.
19. Arshavsky, V. Y., and Bownds, M. D. (1992) *Nature* 357, 416–417.
20. Angleson, J. K., and Wensel, T. G. (1993) *Neuron* 11, 939–949.
21. Arshavsky, V. Y., Dumke, C. L., Zhu, Y., Artemyev, N. O., Skiba, N. P., Hamm, H. E., and Bownds, M. D. (1994) *J. Biol. Chem.* 269, 19882–19887.
22. Chen, C. K., Wieland, T., and Simon, M. I. (1996) *Proc. Natl. Acad. Sci. U.S.A.* 93, 12885–12889.
23. Faurobert, E., and Hurley, J. B. (1997) *Proc. Natl. Acad. Sci. U.S.A.* 94, 2945–2950.
24. He, W., Cowan, C. W., and Wensel, T. G. (1998) *Neuron* 20, 95–102.
25. Cowan, C. W., Fariss, R. N., Sokal, I., Palczewski, K., and Wensel, T. G. (1998) *Proc. Natl. Acad. Sci. U.S.A.* 95, 5351–5356.
26. Wieland, T., Chen, C.-K., and Simon, M. I. (1997) *J. Biol. Chem.* 271, 8853–8856.
27. Natochin, M., Granovsky, A. E., and Artemyev, N. O. (1997) *J. Biol. Chem.* 272, 17444–17449.
28. Nekrasova, E. R., Berman, D. M., Rustandi, R. R., Hamm, H. E., Gilman, A. G., and Arshavsky, V. Y. (1997) *Biochemistry* 36, 7638–7643.
29. Papermaster, D. S., and Dreyer, W. J. (1974) *Biochemistry* 13, 2438–2444.
30. Yamanaka, G., Eckstein, F., and Stryer, L. (1985) *Biochemistry* 24, 8094–8101.
31. Stryer, L., Hurley, J. B., and Fung, B. K.-K. (1983) *Methods Enzymol.* 96, 617–627.
32. Skiba, N. P., Artemyev, N. O., and Hamm, H. E. (1995) *J. Biol. Chem.* 270, 13210–13215.

33. Guan, K., and Dixon, J. E. (1991) *Anal. Biochem.* 192, 262–267.
34. Bradford, M. M. (1976) *Anal. Biochem.* 72, 248–254.
35. Peitsch, M. C. (1996) *Biochem. Soc. Trans.* 24, 274–279.
36. Lipkin, V. M., Dumler, I. L., Muradov, K. G., Artemyev, N. O., and Etingof, R. N. (1988) *FEBS Lett.* 234, 287–290.
37. Artemyev, N. O., Rarick, H. M., Mills, J. S., Skiba, N. P., and Hamm, H. E. (1992) *J. Biol. Chem.* 267, 25067–25072.
38. Brown, R. L. (1992) *Biochemistry* 31, 5918–5925.
39. Blackwell, J. R., and Horgan, R. (1991) *FEBS Lett.* 295, 10–12.
40. Natochin, M., Granovsky, A. E., and Artemyev, N. O. (1998) *J. Biol. Chem.* 273, 21808–21815.
41. Artemyev, N. O. (1997) *Biochemistry* 36, 4188–4193.

BI982636X